PHYSICAL REVIEW C **95**, 031601(R) (2017)

How the Pauli exclusion principle affects fusion of atomic nuclei

C. Simenel,[1,*] A. S. Umar,[2,†] K. Godbey,[2,‡] M. Dasgupta,[1] and D. J. Hinde[1]

[1]*Department of Nuclear Physics, Research School of Physics and Engineering, The Australian National University, Canberra ACT 2601, Australia*

[2]*Department of Physics and Astronomy, Vanderbilt University, Nashville, Tennessee 37235, USA*

(Received 16 October 2016; revised manuscript received 8 January 2017; published 2 March 2017)

The Pauli exclusion principle induces a repulsion between composite systems of identical fermions such as colliding atomic nuclei. Our goal is to study how heavy-ion fusion is impacted by this "Pauli repulsion." We propose a new microscopic approach, the density-constrained frozen Hartree-Fock method, to compute the bare potential including the Pauli exclusion principle exactly. Pauli repulsion is shown to be important inside the barrier radius and increases with the charge product of the nuclei. Its main effect is to reduce tunneling probability. Pauli repulsion is part of the solution to the long-standing deep sub-barrier fusion hindrance problem.

DOI: 10.1103/PhysRevC.95.031601

The idea that identical fermions cannot occupy the same quantum state was proposed by Stoner [1] and generalized by Pauli [2]. Known as the Pauli exclusion principle, it was at first empirical, but is now explained by the spin-statistic theorem in quantum field theory [3,4]. The importance of the Pauli exclusion principle cannot be overstated. For instance, it is largely responsible for the stability of matter against collapse, as demonstrated by the existence of white dwarfs. It is also expected to play a crucial role in the dynamics of systems of identical fermions. For instance, it could impact quantum tunneling of complex systems which remains one of the greatest challenges of the quantum many-body problem. This work addresses the question of the effect of the Pauli exclusion principle on tunneling of complex systems in the specific framework of nuclear physics which offers an ideal ground to test concepts of the quantum many-body problem.

The Pauli exclusion principle generates a repulsion between composite systems of identical fermions at short distance. For example, it repels atomic electron clouds in ionic molecules due to the fermionic nature of the electron. Another example is the hard-core repulsion between two nucleons induced by identical quarks of the same color present in both nucleons. Naturally, a similar effect is expected to occur between atomic nuclei which are composite systems of nucleons. Indeed, it has been predicted that the Pauli exclusion principle should induce a repulsion (called "Pauli repulsion" hereafter) between strongly overlapping nuclei [5].

The Pauli repulsion should then be included in the nucleus-nucleus potentials used to model reactions such as (in)elastic scattering, (multi)nucleon transfer, and fusion. However, Pauli repulsion is usually neglected in these models. It has been argued that the outcome of a collision between nuclei is mostly determined at a distance where the nuclei do not overlap much and thus the effects of the Pauli exclusion principle are minimized. This argument is based on the assumption that nuclei do not necessarily probe the inner part of the fusion barrier. However, at energies well above the barrier, the system could reach more compact shapes where one cannot neglect the effect of the Pauli principle anymore, as was shown by several authors in the 1970s [5–9]. Similarly, for deep sub-barrier energies the inner turning point of the fusion barrier entails significant overlap between the two nuclei [10,11].

Using a realistic microscopic approach to compute nucleus-nucleus bare potentials, we show that, in fact, Pauli repulsion plays an important role in fusion at deep sub-barrier energies. In particular, it provides a natural (though only partial) explanation for the experimentally observed deep sub-barrier fusion hindrance [12–14] (see Ref. [15] for a review) which has led to various theoretical interpretations [13,16–21], although none of them directly consider Pauli repulsion as a possible mechanism.

To investigate the effect of Pauli repulsion on heavy-ion fusion, we introduce a novel microscopic method called the density-constrained frozen Hartree-Fock (DCFHF) method to compute the interaction between nuclei while accounting exactly for the Pauli exclusion principle between nucleons. The microscopically derived bare nucleus-nucleus potential including Pauli repulsion is then used to study deep sub-barrier fusion. For simplicity, we focus on systems with doubly magic nuclei which are spherical and nonsuperfluid. As an example, $^{16}\mathrm{O}+{}^{16}\mathrm{O}$, $^{40,48}\mathrm{Ca}+{}^{40,48}\mathrm{Ca}$, $^{16}\mathrm{O}+{}^{208}\mathrm{Pb}$, and $^{48}\mathrm{Ca}+{}^{208}\mathrm{Pb}$ reactions are studied theoretically and compared with experimental data.

To avoid the introduction of new parameters, we adopt the idea of Brueckner *et al.* [22] to derive the bare potential from an energy density functional (EDF) $E[\rho]$ written as an integral of an energy density $\mathcal{H}[\rho(\mathbf{r})]$, i.e.,

$$E[\rho] = \int d\mathbf{r}\ \mathcal{H}[\rho(\mathbf{r})]. \tag{1}$$

The bare potential is obtained by requiring frozen ground-state densities ρ_i of each nucleus ($i = 1,2$) which we compute using the Hartree-Fock (HF) mean-field approximation [23,24]. The Skyrme EDF [25] is used both in HF calculations and to compute the bare potential. It accounts for the bulk properties of nuclear matter such as its incompressibility, which is crucial at short distances [16,22,26]. Neglecting the Pauli exclusion principle between nucleons in different nuclei leads to the

*cedric.simenel@anu.edu.au
†umar@compsci.cas.vanderbilt.edu
‡kyle.s.godbey@vanderbilt.edu

usual frozen Hartree-Fock (FHF) potential [27–30]

$$V_{\rm FHF}(\mathbf{R}) = \int d\mathbf{r}\ \mathcal{H}[\rho_1(\mathbf{r}) + \rho_2(\mathbf{r}-\mathbf{R})] - E[\rho_1] - E[\rho_2], \tag{2}$$

where $\mathbf{R}$ is the distance vector between the centers of mass of the nuclei. The FHF potential, assumed to be central, can then directly be used to compute fusion cross sections [31–33].

Our new DCFHF method is the static counterpart of the density-constrained time-dependent Hartree-Fock approach developed to extract the nucleus-nucleus potential of dynamically evolving systems [34] (see also Refs. [35,36]). In particular, this approach shows that the Pauli exclusion principle splits orbitals such that some states contribute attractively (bounding) and some repulsively (antibounding) to the potential [37]. To disentangle effects of the Pauli exclusion principle from the dynamics, we need to investigate the bare potential without polarization effects. The dynamics can be included in a second step via, e.g., coupled-channel [31] or TDHF [28,38,39] calculations. A discussion about the use of DCFHF potentials in coupled-channel calculations can be found in the Supplemental Material (Ref. [40]).

In the present method, it is important that the nuclear densities remain frozen as the densities of the HF ground states of the collision partners. Consequently, the DCFHF approach facilitates the computation of the bare potential by using the self-consistent HF mean field with exact frozen densities. The Pauli exclusion principle is included exactly by allowing the single-particle states, comprising the combined nuclear density, to reorganize to attain their minimum energy configuration and be properly antisymmetrized as the many-body state is a Slater determinant of all the occupied single-particle wave functions. The HF minimization of the combined system is thus performed subject to the constraint that the local proton p and neutron n densities do not change:

$$\delta\left\langle H - \sum_{q=p,n}\int d\mathbf{r}\ \lambda_q(\mathbf{r})\,[\rho_{1_q}(\mathbf{r}) + \rho_{2_q}(\mathbf{r}-\mathbf{R})]\right\rangle = 0, \tag{3}$$

where the $\lambda_{n,p}(\mathbf{r})$ are Lagrange parameters at each point of space constraining the neutron and proton densities. See Supplemental Material (Ref. [40]) for details of the implementation of the DCFHF method. This equation determines the state vector (Slater determinant) $|\Phi(\mathbf{R})\rangle$. The DCFHF potential, assumed to be central, is then defined as

$$V_{\rm DCFHF}(R) = \langle\Phi(\mathbf{R})|H|\Phi(\mathbf{R})\rangle - E[\rho_1] - E[\rho_2]. \tag{4}$$

The FHF and DCFHF calculations of bare nucleus-nucleus potentials were done in a three-dimensional Cartesian geometry with no symmetry assumptions using a static version of the code of Ref. [41] and using the Skyrme SLy4d interaction [42], which has been successful in describing various types of nuclear reactions [30]. The three-dimensional Poisson equation for the Coulomb potential is solved by using fast-Fourier transform techniques and the Slater approximation is used for the Coulomb exchange term. The static HF equations and the DCFHF minimizations are implemented using the damped gradient iteration method. The box size used for all the calculations was chosen to be $60 \times 30 \times 30$ fm^3, with a mesh spacing of 1.0 fm in all directions. These values provide very accurate results due to the employment of sophisticated discretization techniques [43,44].

The FHF (solid line) and DCFHF (dashed line) potentials are shown in Figs. 1(a)–1(c) for ^{40}Ca + ^{40}Ca, ^{48}Ca + ^{48}Ca, and ^{16}O + ^{208}Pb systems, respectively. We observe that the Pauli exclusion principle (present only in DCFHF) induces a repulsion at short distance in the three systems. The resulting effects are negligible outside the barrier and relatively modest near the barrier. However, the impact is more important in the inner barrier region, with the production of a potential pocket at short distance. Interestingly, the most important effect of Pauli repulsion is to increase the barrier width. It is then expected to reduce the sub-barrier tunneling probability as the latter decreases exponentially with the barrier width.

The impact of Pauli repulsion on the nucleus-nucleus potential varies with the systems. In ^{16}O + ^{16}O (see Fig. 2), the pocket height is negative and Pauli repulsion is expected to have a small impact on fusion in this system, except potentially at astrophysical energies. However, the pocket becomes shallower with increasing charge product Z_1Z_2 and almost disappears in ^{48}Ca+^{208}Pb (see Fig. 3). This is consistent with the fact that more nuclear overlap (and thus a larger Pauli repulsion) is required to compensate for the larger Coulomb repulsion between the fragments. However, the two-body picture for such heavy systems is questionable. Figure 3 shows indeed an extreme case where the DCFHF calculation predicts that fusion is impossible at 3% below the barrier. In fact, a smooth transition toward an adiabatic potential for the compound system is expected [20] which would allow fusion to occur at lower energies. Finally, the Pauli repulsion not only depends on Z_1Z_2, but also on the number of neutrons. This is illustrated in Fig. 4 which compares the DCFHF potentials for the three ^{40,48}Ca + ^{40,48}Ca systems. At touching distance, additional neutrons increase the barrier radius (due to the neutron skin) and thus decrease its height. For this reason, ^{48}Ca + ^{48}Ca has the lowest barrier and ^{40}Ca + ^{40}Ca the largest one. However, ^{48}Ca + ^{48}Ca also exhibits the strongest Pauli repulsion of the three systems. This is interpreted as an effect of the larger number of neutrons overlapping at short distance, thus increasing the Pauli repulsion. Note also that, once the dynamics is included, fusion in these systems may behave differently and static effects on the bare potential could be washed out by the dynamics [33]. In particular, fusion in the ^{40}Ca + ^{48}Ca system is expected to be strongly affected by transfer channels [47,49], a feature which has only recently been studied in a microscopic approach [50].

In principle, the Pauli repulsion is expected to be energy dependent. One source of energy dependence is the diminishing of the overlap between wave functions with relative kinetic momenta at higher energies reducing the Pauli repulsion [5,6,8,51]. Other sources are the dependence of the EDF on the current density (needed for Galilean invariance) [6] and nonlocal effects of the Pauli exclusion principle leading to an energy dependence of the local equivalent potential [52,53]. These effects, however, are expected to impact the Pauli repulsion at energies much higher than

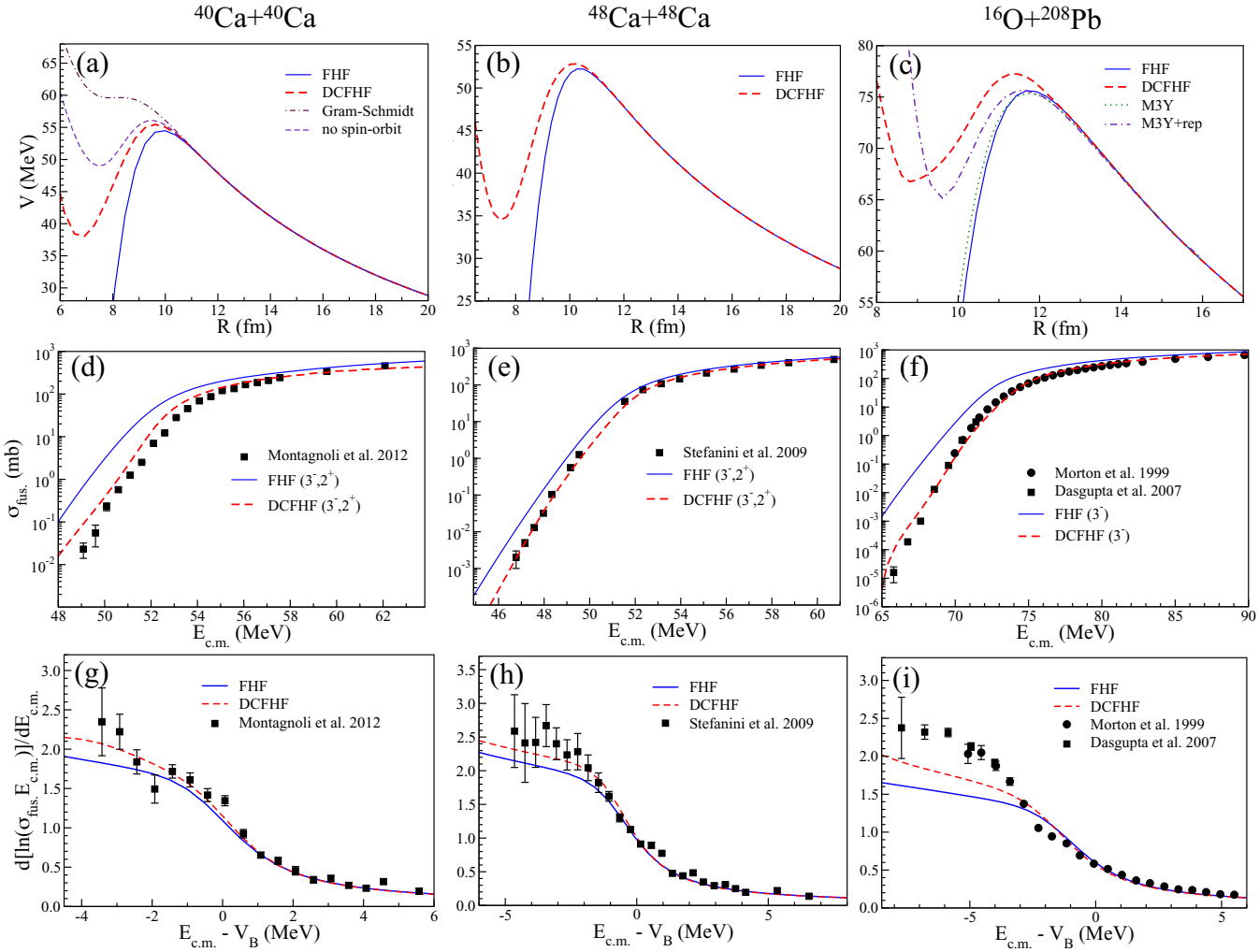

FIG. 1. (a)–(c) Nucleus-nucleus potential without (FHF) and with (DCFHF) Pauli exclusion principle between nucleons of different nuclei. Potentials from a Gram-Schmidt antisymmetrization (dotted-dashed line) and from DCFHF without rearrangement of the spin-orbit density (thin dashed line) are shown in (a). M3Y (dotted line) and M3Y+rep (dotted-dashed line) phenomenological potentials [45] are shown in (c). (d)–(f) Experimental [13,46–48] and theoretical (coupled-channel calculations with couplings to low-lying collective 2^+ and/or 3^- states) fusion cross sections $\sigma_{\rm fus}$ vs center-of-mass energy $E_{\rm c.m.}$. (g)–(i) Logarithmic slopes of $\sigma_{\rm fus}E_{\rm c.m.}$ vs $E_{\rm c.m.} - V_B$ where V_B is the barrier energy. In (g)–(i), FHF and DCFHF cross sections are obtained without couplings, the latter being included via a shift in $E_{\rm c.m.}$ (see text).

the barrier (at least twice the barrier energy in $^{16}O + ^{16}O$ [5,6]), and can then be neglected in near-barrier fusion studies.

We have also tested other methods to account for Pauli repulsion in the bare potential. For instance, antisymmetrizing overlapping ground-state wave functions [5–7] can be done with a Gram-Schmidt procedure. Although the resulting potential properly accounts for the Pauli exclusion principle, it leads to much higher repulsion as illustrated in Fig. 1(a) (dotted-dashed line) for the $^{40}Ca + ^{40}Ca$ system in which the potential pocket and therefore the fusion barrier simply disappear. Let us use a simple model to explain the origin of this large repulsion. Consider two single-particle wave functions $\varphi_{1,2}$ belonging to the HF ground states of the two different nuclei and which have a small overlap in the neck region at $\mathbf{r}_0$ only: $\varphi_1^*(\mathbf{r})\varphi_2(\mathbf{r}) \simeq \alpha\delta(\mathbf{r} - \mathbf{r}_0)$. By definition, the total frozen density of these two nucleons is $\rho_F = |\varphi_1|^2 + |\varphi_2|^2$. The evaluation of observables, however, requires antisymmetrized wave functions such as $\tilde{\varphi}_\pm = \mathcal{N}_\pm(\varphi_1 \pm \varphi_2)$ with normalization coefficients $\mathcal{N}_\pm = (2 \pm \alpha \pm \alpha^*)^{-1/2}$ and overlaps $\langle\tilde{\varphi}_-|\tilde{\varphi}_+\rangle = 0$. The corresponding density reads

$$\tilde{\rho} = |\tilde{\varphi}_+|^2 + |\tilde{\varphi}_-|^2 \simeq \rho_F - \tfrac{1}{2}(\alpha + \alpha^*)^2\delta(\mathbf{r} - \mathbf{r}_0).$$

It is reduced in the neck compared to the frozen density and thus leads to a smaller nuclear attraction between the nuclei or, equivalently, to a spurious repulsion between the fragments as seen in Fig. 1(a). Naive antisymmetrization procedures are then not compatible with the frozen density picture. This was also recognized in the earlier work concerning α-nucleus scattering studies [54], where specialized normalization operators were developed to reconstruct the states following a Gram-Schmidt orthogonalization. However, these methods could only be applied using semianalytic methods. The DCFHF achieves this without any approximation. These methods have also

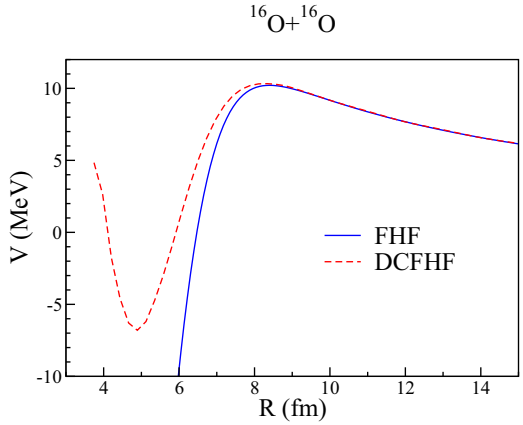

FIG. 2. $^{16}\mathrm{O}+{}^{16}\mathrm{O}$ nucleus-nucleus potential without (FHF) and with (DCFHF) Pauli exclusion principle between nucleons of different nuclei.

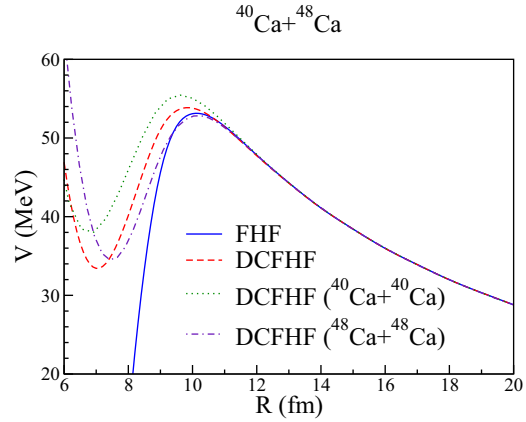

FIG. 4. Same as Fig. 2, but for $^{40}\mathrm{Ca}+{}^{48}\mathrm{Ca}$. DCFHF potentials of the other ^{A}Ca + ^{A}Ca are also reported.

been subsequently criticized by groups performing resonating group method (RGM) calculations [55–58]. In principle, RGM does provide a theoretical approach to constructing internuclear potentials with full antisymmetrization. However, such calculations have thus far been limited to light systems and direct reactions due to their complexity.

Let us now discuss another traditional method which is to account for Pauli repulsion simply by increasing the kinetic energy density $\tau(\mathbf{r})$ (e.g., via the Thomas-Fermi model) [6–8,59,60]. This method would be valid if the effect of the Pauli exclusion principle was only to rearrange the kinetic energy term $\frac{\hbar^2}{2m}\tau$ without impacting other terms of the functional. In fact, the EDF also depends on τ via the "$t_{1,2}$" momentum-dependent terms of the Skyrme effective interaction [25] and, then, a variation of $\tau(\mathbf{r})$ also affects the nuclear part of the potential [6,59]. At the same time, we have also observed that including the Pauli exclusion principle has a strong impact on the spin-orbit energy. This is illustrated in Fig. 1(a) for the $^{40}\mathrm{Ca}+{}^{40}\mathrm{Ca}$ system. For this system, removing the spin-orbit interaction in the FHF potential (not shown in the figure) has little effect, but strongly increases the repulsion between the fragments in the DCFHF potential (thin dashed line). This shows that the spin-orbit energy absorbs a large part of the Pauli repulsion. Thus, the Pauli exclusion principle has a more complicated effect than just increasing the kinetic energy.

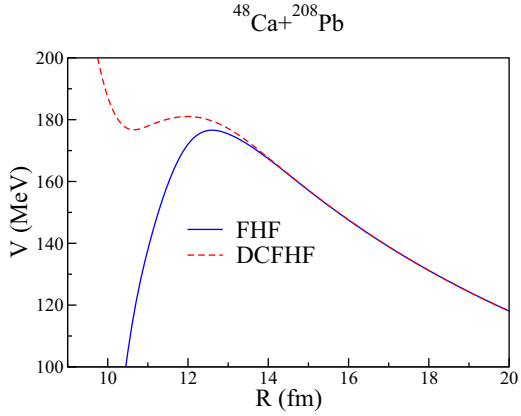

FIG. 3. Same as Fig. 2, but for $^{48}\mathrm{Ca}+{}^{208}\mathrm{Pb}$.

Coupled-channel calculations of fusion cross sections were performed with the CCFULL code [61] using Woods-Saxon fits of the FHF and DCFHF potentials. By default, the incoming wave boundary condition (IWBC) was used. For shallow pocket potentials, however, the IWBC should be replaced by an imaginary potential at the potential pocket to avoid numerical instabilities. This is done for calculations with the $^{16}\mathrm{O}+{}^{208}\mathrm{Pb}$ DCFHF potential using a modified version of CCFULL with Woods-Saxon parameters $\{V_I = 30$ MeV, $a_I = 1$ fm, $r_I = 0.3$ fm$\}$ for the imaginary potential. Couplings to the low-lying collective 2^+ (in calcium isotopes) and 3^- states are included with standard values of the coupling constants [46,62]. In CCFULL, one (two) vibrational mode(s) can be included in the projectile (target). For the 2^+ states, we then use the fact that, for symmetric systems, the mutual excitation of one-phonon states in both nuclei can be approximated by one phonon with a coupling constant scaled by $\sqrt{2}$ [63]. Here, the CC calculations are kept simple and include only the most relevant couplings. Improvements could be obtained, e.g., by including anharmonicity of the multiphonon states [64]. The resulting fusion cross sections are plotted in Figs. 1(d)–1(f). Calculations with the FHF potential systematically overestimate the data, while the DCFHF potential leads to a much better agreement with experiment at all energies and ranging over eight orders of magnitude in cross sections. This shows the importance of taking into account Pauli repulsion in the bare potential for fusion calculations. We emphasize that these calculations are performed without adjustable parameters.

The behavior of fusion at deep sub-barrier energies is often studied using the logarithmic slope $d\ln(\sigma_{\mathrm{fus}}E_{\mathrm{c.m.}})/dE_{\mathrm{c.m.}}$. Large logarithmic slopes are a signature of a rapid decrease of σ_{fus} with decreasing energy. Deep sub-barrier fusion hindrance is characterized by the failure of theoretical models to reproduce large logarithmic slopes observed experimentally at low energy. To avoid numerical instabilities due to shallow potentials in the calculations of logarithmic slopes, couplings

to internal excitations of the nuclei have been removed in the calculations of barrier transmission and accounted for via an overall lowering of V_B by less than 5% depending on the structure of the reactants [13]. Indeed, it has been shown that couplings have little effect on the logarithmic slope at these energies [13]. We see in Figs. 1(g)–1(i) that the inclusion of Pauli repulsion in DCFHF indeed increases the logarithmic slope at low energy. Although Pauli repulsion is shown to play a crucial role, it is not yet sufficient to reproduce experimental data at deep sub-barrier energies. Other contributions are expected to come from dissipative effects [13] and from the transition between the nucleus-nucleus potential to the one-nucleus adiabatic potential [20]. However, repulsive effects from the incompressibility of nuclear matter invoked in [16] are not observed in our microscopic calculations. Both the FHF and DCFHF calculations use the same Skyrme functional (SLy4d) with a realistic compression modulus of the symmetric nuclear matter $K_\infty \simeq 230$ MeV. Although the FHF potential properly takes into account effects due to incompressibility, it is very close to standard phenomenological potentials. We illustrate this with the example of the M3Y potential [16] in Fig. 1(c). The addition of a repulsive component at short distance [M3Y+rep parametrization shown with a dotted-dashed line Fig. 1(c)], introduced phenomenologically in [16] to explain experimental fusion data at deep sub-barrier energies, then cannot be justified by an effect of incompressibility. It is more likely that it simulates other effects such as Pauli repulsion.

C.S. thanks E. C. Simpson for useful discussions. This work has been supported by the Australian Research Council Grant No. FT120100760, and by the U.S. Department of Energy under Grant No. DE-SC0013847 with Vanderbilt University.

[1] E. C. Stoner, The distribution of electrons among atomic levels, Phil. Mag. **48**, 719 (1924).
[2] W. Pauli, Über den zusammenhang des abschlusses der elektronengruppen im atom mit der komplexstruktur der spektren, Z. Phys. **31**, 765 (1925).
[3] M. Fierz, Über die relativistische theorie krftefreier teilchen mit beliebigem spin, Helv. Phys. Acta **12**, 3 (1939).
[4] W. Pauli, The connection between spin and statistics, Phys. Rev. **58**, 716 (1940).
[5] T. Fliessbach, The optical potential for the elastic heavy ion scattering, Z. Phys. **247**, 117 (1971).
[6] D. M. Brink and F. Stancu, Interaction potential between two ^{16}O nuclei derived from the Skyrme interaction, Nucl. Phys. A **243**, 175 (1975).
[7] P. G. Zint and U. Mosel, Kinetic energy contributions to heavy ion potentials, Phys. Lett. B **56**, 424 (1975).
[8] F. Beck, K.-H. Müller, and H. S. Köhler, Momentum Dependence of the Ion-Ion Potential in a Microscopic Theory, Phys. Rev. Lett. **40**, 837 (1978).
[9] B. Sinha and S. A. Moszkowski, The nucleus-nucleus interaction potential using density-dependent delta interaction, Phys. Lett. B **81**, 289 (1979).
[10] C. H. Dasso and G. Pollarolo, Investigating the nucleus-nucleus potential at very short distances, Phys. Rev. C **68**, 054604 (2003).
[11] A. S. Umar, V. E. Oberacker, and C. J. Horowitz, Microscopic sub-barrier fusion calculations for the neutron star crust, Phys. Rev. C **85**, 055801 (2012).
[12] C. L. Jiang, H. Esbensen, K. E. Rehm, B. B. Back, R. V. F. Janssens, J. A. Caggiano, P. Collon, J. Greene, A. M. Heinz, D. J. Henderson, I. Nishinaka, T. O. Pennington, and D. Seweryniak, Unexpected Behavior of Heavy-Ion Fusion Cross Sections at Extreme Sub-Barrier Energies, Phys. Rev. Lett. **89**, 052701 (2002).
[13] M. Dasgupta, D. J. Hinde, A. Diaz-Torres, B. Bouriquet, C. I. Low, G. J. Milburn, and J. O. Newton, Beyond the Coherent Coupled Channels Description of Nuclear Fusion, Phys. Rev. Lett. **99**, 192701 (2007).
[14] A. M. Stefanini, G. Montagnoli, L. Corradi, S. Courtin, E. Fioretto, A. Goasduff, F. Haas, P. Mason, R. Silvestri, P. P. Singh, F. Scarlassara, and S. Szilner, Fusion hindrance for ^{58}Ni + ^{54}Fe, Phys. Rev. C **82**, 014614 (2010).
[15] B. B. Back, H. Esbensen, C. L. Jiang, and K. E. Rehm, Recent developments in heavy-ion fusion reactions, Rev. Mod. Phys. **86**, 317 (2014).
[16] Ş. Mişicu and H. Esbensen, Hindrance of Heavy-Ion Fusion due to Nuclear Incompressibility, Phys. Rev. Lett. **96**, 112701 (2006).
[17] Ş. Mişicu and H. Esbensen, Signature of shallow potentials in deep sub-barrier fusion reactions, Phys. Rev. C **75**, 034606 (2007).
[18] A. Diaz-Torres, D. J. Hinde, M. Dasgupta, G. J. Milburn, and J. A. Tostevin, Dissipative quantum dynamics in low-energy collisions of complex nuclei, Phys. Rev. C **78**, 064604 (2008).
[19] A. Diaz-Torres, Coupled-channels density-matrix approach to low-energy nuclear collision dynamics: A technique for quantifying quantum decoherence effects on reaction observables, Phys. Rev. C **82**, 054617 (2010).
[20] T. Ichikawa, K. Hagino, and A. Iwamoto, Signature of Smooth Transition from Sudden to Adiabatic States in Heavy-Ion Fusion Reactions at Deep Sub-Barrier Energies, Phys. Rev. Lett. **103**, 202701 (2009).
[21] T. Ichikawa, Systematic investigations of deep sub-barrier fusion reactions using an adiabatic approach, Phys. Rev. C **92**, 064604 (2015).
[22] K. A. Brueckner, J. R. Buchler, and M. M. Kelly, New theoretical approach to nuclear heavy-ion scattering, Phys. Rev. **173**, 944 (1968).
[23] D. R. Hartree, The wave mechanics of an atom with a non-Coulomb central field. Part I. Theory and methods, Proc. Camb. Phil. Soc. **24**, 89 (1928).
[24] V. A. Fock, Näherungsmethode zur lösung des quantenmechanischen mehrkörperproblems, Z. Phys. **61**, 126 (1930).
[25] T. H. R. Skyrme, CVII. The nuclear surface, Phil. Mag. **1**, 1043 (1956).
[26] S. Hossain, A. S. B. Tariq, A. Nilima, M. S. Islam, R. Majumder, M. A. Sayed, M. M. Billah, M. M. B. Azad, M. A. Uddin, I. Reichstein, F. B. Malik, and A. K. Basak, Dependence of the ^{16}O + ^{16}O nuclear potential on nuclear incompressibility, Phys. Rev. C **91**, 064613 (2015).
[27] V. Y. Denisov and W. Nörenberg, Entrance channel potentials in the synthesis of the heaviest nuclei, Eur. Phys. J. A **15**, 375 (2002).

[28] K. Washiyama and D. Lacroix, Energy dependence of the nucleus-nucleus potential close to the Coulomb barrier, Phys. Rev. C **78**, 024610 (2008).
[29] C. Simenel and B. Avez, Time-dependent Hartree-Fock description of heavy ions fusion, Intl. J. Mod. Phys. E **17**, 31 (2008).
[30] C. Simenel, Nuclear quantum many-body dynamics, Eur. Phys. J. A **48**, 152 (2012).
[31] C. Simenel, M. Dasgupta, D. J. Hinde, and E. Williams, Microscopic approach to coupled-channels effects on fusion, Phys. Rev. C **88**, 064604 (2013).
[32] D. Bourgin, C. Simenel, S. Courtin, and F. Haas, Microscopic study of ^{40}Ca + ^{58,64}Ni fusion reactions, Phys. Rev. C **93**, 034604 (2016).
[33] K. Vo-Phuoc, C. Simenel, and E. C. Simpson, Dynamical effects in fusion with exotic nuclei, Phys. Rev. C **94**, 024612 (2016).
[34] A. S. Umar and V. E. Oberacker, Heavy-ion interaction potential deduced from density-constrained time-dependent Hartree-Fock calculation, Phys. Rev. C **74**, 021601 (2006).
[35] R. Y. Cusson, P.-G. Reinhard, M. R. Strayer, J. A. Maruhn, and W. Greiner, Density as a constraint and the separation of internal excitation energy in TDHF, Z. Phys. A **320**, 475 (1985).
[36] A. S. Umar, M. R. Strayer, R. Y. Cusson, P.-G. Reinhard, and D. A. Bromley, Time-dependent Hartree-Fock calculations of ^{4}He + ^{14}C,^{12}C + ^{12}C(0^{+}), and ^{4}He + ^{20}Ne molecular formations, Phys. Rev. C **32**, 172 (1985).
[37] A. S. Umar, V. E. Oberacker, J. A. Maruhn, and P.-G. Reinhard, Microscopic composition of ion-ion interaction potentials, Phys. Rev. C **85**, 017602 (2012).
[38] C. Simenel, R. Keser, A. S. Umar, and V. E. Oberacker, Microscopic study of ^{16}O + ^{16}O fusion, Phys. Rev. C **88**, 024617 (2013).
[39] A. S. Umar, C. Simenel, and V. E. Oberacker, Energy dependence of potential barriers and its effect on fusion cross sections, Phys. Rev. C **89**, 034611 (2014).
[40] See Supplemental Material at http://link.aps.org/supplemental/10.1103/PhysRevC.95.031601 for details of the implementation of the DCFHF method to compute nucleus-nucleus potentials and discussion of its use in coupled-channel calculations.
[41] A. S. Umar and V. E. Oberacker, Three-dimensional unrestricted time-dependent Hartree-Fock fusion calculations using the full Skyrme interaction, Phys. Rev. C **73**, 054607 (2006).
[42] K. Kim, T. Otsuka, and P. Bonche, Three-dimensional TDHF calculations for reactions of unstable nuclei, J. Phys. G **23**, 1267 (1997).
[43] A. S. Umar, M. R. Strayer, J. S. Wu, D. J. Dean, and M. C. Güçlü, Nuclear Hartree-Fock calculations with splines, Phys. Rev. C **44**, 2512 (1991).
[44] A. S. Umar, J. Wu, M. R. Strayer, and C. Bottcher, Basis-spline collocation method for the lattice solution of boundary value problems, J. Comp. Phys. **93**, 426 (1991).
[45] H. Esbensen and Ş. Mişicu, Hindrance of ^{16}O + ^{208}Pb fusion at extreme sub-barrier energies, Phys. Rev. C **76**, 054609 (2007).
[46] C. R. Morton, A. C. Berriman, M. Dasgupta, D. J. Hinde, J. O. Newton, K. Hagino, and I. J. Thompson, Coupled-channels analysis of the ^{16}O + ^{208}Pb fusion barrier distribution, Phys. Rev. C **60**, 044608 (1999).
[47] G. Montagnoli, A. M. Stefanini, C. L. Jiang, H. Esbensen, L. Corradi, S. Courtin, E. Fioretto, A. Goasduff, F. Haas, A. F. Kifle, C. Michelagnoli, D. Montanari, T. Mijatoviç, K. E. Rehm, R. Silvestri, P. P. Singh, F. Scarlassara, S. Szilner, X. D. Tang, and C. A. Ur, Fusion of ^{40}Ca + ^{40}Ca and other Ca + Ca systems near and below the barrier, Phys. Rev. C **85**, 024607 (2012).
[48] A. M. Stefanini, G. Montagnoli, R. Silvestri, L. Corradi, S. Courtin, E. Fioretto, B. Guiot, F. Haas, D. Lebhertz, P. Mason, F. Scarlassara, and S. Szilner, How does fusion hindrance show up in medium-light systems? The case of ^{48}Ca + ^{48}Ca, Phys. Lett. B **679**, 95 (2009).
[49] C. L. Jiang, A. M. Stefanini, H. Esbensen, K. E. Rehm, L. Corradi, E. Fioretto, P. Mason, G. Montagnoli, F. Scarlassara, R. Silvestri, P. P. Singh, S. Szilner, X. D. Tang, and C. A. Ur, Fusion hindrance for Ca + Ca systems: Influence of neutron excess, Phys. Rev. C **82**, 041601 (2010).
[50] K. Godbey, A. S. Umar, and C. Simenel, Dependence of fusion on isospin dynamics, Phys. Rev. C **95**, 011601 (2017).
[51] G.-H. Göritz and U. Mosel, Optical potentials for elastic heavy ion scattering, Z. Phys. A **277**, 243 (1976).
[52] E. W. Schmid, S. Saito, and H. Fiedeldey, The concept of a Pauli barrier in nucleus-nucleus scattering, Z. Phys. A **306**, 37 (1982).
[53] L. C. Chamon, B. V. Carlson, L. R. Gasques, D. Pereira, C. De Conti, M. A. G. Alvarez, M. S. Hussein, M. A. Cândido Ribeiro, E. S. Rossi, Jr., and C. P. Silva, Toward a global description of the nucleus-nucleus interaction, Phys. Rev. C **66**, 014610 (2002).
[54] T. Fliessbach, The reduced width amplitude in the reaction theory for composite particles, Z. Phys. A **272**, 39 (1975).
[55] K. Aoki and H. Horiuchi, Study of local inter-nucleus potential on the basis of the resonating group method. IV: Comparison of various approaches to calculate inter-nucleus potential and study of the origins of deep and shallow potentials, Prog. Theor. Phys. **69**, 1154 (1983).
[56] T. Wada and H. Horiuchi, Comparison of the Microscopic Potential with the Optical Potential in the α + ^{16}O System, Phys. Rev. Lett. **58**, 2190 (1987).
[57] A. Tohsaki, F. Tanabe, and R. Tamagaki, Microscopic study of ^{16}O − ^{16}O interaction by the resonating group method, Prog. Theor. Phys. **53**, 1022 (1975).
[58] Y. C. Tang, M. LeMere, and D. R. Thompsom, Resonating group method for nuclear many-body problems, Phys. Rep. **47**, 167 (1978).
[59] V. Y. Denisov and V. A. Nesterov, Effect of the Pauli exclusion principle on the potential of nucleus-nucleus interaction, Phys. At. Nucl. **73**, 1142 (2010).
[60] V. A. Nesterov, Effect of the Pauli exclusion principle and the polarization of nuclei on the potential of their interaction for the example of the ^{16}O + ^{16}O system, Phys. At. Nucl. **76**, 577 (2013).
[61] K. Hagino, N. Rowley, and A. Kruppa, A program for coupled-channel calculations with all order couplings for heavy-ion fusion reactions, Comput. Phys. Commun. **123**, 143 (1999).
[62] N. Rowley and K. Hagino, Entrance-channel effects in heavy-ion capture: role of octupole phonons, Nucl. Phys. A **834**, 110c (2010).
[63] H. Esbensen and S. Landowne, Higher-order coupling effects in low energy heavy-ion fusion reactions, Phys. Rev. C **35**, 2090 (1987).
[64] J. M. Yao and K. Hagino, Anharmonicity of multi-octupole-phonon excitations in ^{208}Pb: Analysis with multireference covariant density functional theory and subbarrier fusion of ^{16}O + ^{208}Pb, Phys. Rev. C **94**, 011303 (2016).